ELSEVIER

Journal of Nuclear Materials 254 (1998) 205–214

journal of nuclear materials

Permeation of multi-component hydrogen isotopes through nickel

Tomofumi Shiraishi *, Masabumi Nishikawa, Teruki Fukumatsu

Department of Nuclear Engineering, Faculty of Engineering, Kyushu University, Hakozaki, Higashi-ku, Fukuoka 812-81, Japan

Received 14 April 1997; accepted 4 December 1997

Abstract

The experiments were performed to determine the permeabilities of hydrogen and deuterium for nickel in the temperature range of 473 to 973 K using the co-current double tube method. The isotope effect ratio in permeation was estimated from these permeabilities. Solubility constants of hydrogen and deuterium for nickel calculated from the permeabilities of this study and the diffusivities of the literature data agreed well with previously reported values. The permeation behavior of hydrogen isotopes in the binary-component hydrogen isotopes system was also observed under various conditions and compared with the values from the model calculation. It is concluded in this study that the separation factor in permeation of hydrogen isotopes through nickel coincides with the isotope effect ratio and that the numerical calculation using the finite difference method is applicable to predict the permeation behavior of hydrogen isotopes through the wall of a long tube for single- and multi-component hydrogen isotopes system. © 1998 Elsevier Science B.V.

1. Introduction

Permeabilities of hydrogen isotopes through membrane of nickel have been reported by many authors [1–10] for the single-component hydrogen isotope system. However, there are rather large discrepancies in data reported so far. These discrepancies may be partly due to use of the inadequate driving force, disregard of the temperature distribution formed in permeation membrane, or confusion of the isotope effect ratio with the separation factor in estimation of permeation rate. Only the permeation behavior of H_2 was studied in most of these works and the Robertson's 'best value' [6] which correlates the data of various authors is considered to be appropriate [11]. Only a few investigators have reported the permeabilities of D_2 [1–3,8] and T_2 [9] through nickel and no discussions have been made about the permeation behavior in the multi-component hydrogen isotopes system.

The present authors first measured the permeabilities of H_2 and D_2 in the single-component hydrogen isotope system to obtain the isotope effect ratio in permeation. Then, we measured the permeation rates in the binary-component hydrogen isotopes system and discussed the permeation behavior of mixture of hydrogen isotopes in various conditions comparing with the numerically calculated values. In this study a numerical calculation model using the finite difference method was applied to estimate the effect of change of temperature or partial pressure of hydrogen isotopes in the axial direction of a permeation tube on the permeation behavior following the recommendation in the previous works [12,13].

2. Theory

2.1. Permeation of single-component hydrogen isotope system

When a diffusion process of hydrogen isotopes through the metal wall is the controlling step of permeation, the molar flow rate of a hydrogen isotope X_2 (X means H, D, or T in this study), permeating through the metal mem-

* Corresponding author. Tel.: +81-92 642 3785; fax: +81-92 642 3784; e-mail: shiratne@mbox.nc.kyushu-u.ac.jp.

PII S0022-3115(97)00362-0

brane, Q_X (mol/s), is derived from Fick's law and expressed as follows:

$$Q_X = D_X\left(C_{X_1} - C_{X_2}\right) A/t, \tag{1}$$

where A (m^2) is the effective permeation area, t (m) is the thickness of the permeation membrane, D_X (m^2/s) is the diffusivity, and C_{X_1} and C_{X_2} (mol/m^3) are the solubilities in both surface layers of the membrane. The subscripts 1 and 2 in the above equation indicate the inner and outer channels of a double tube, respectively. The permeation rate, J_X (mol $m/m^2 s$), is determined by

$$J_X = Q_X t/A = D_X\left(C_{X_1} - C_{X_2}\right). \tag{2}$$

For permeation through the wall of a tube with circular cross-section, the effective permeation area is given by

$$A = 2\pi lt/\ln(r_2/r_1), \tag{3}$$

where l (m) is the permeation tube length and r_1 (m) and r_2 (m) are the inner and outer radii of the permeation tube, respectively. When the solubility of hydrogen isotope in metal follows Sieverts' law, Eq. (2) is expressed as follows using the partial pressure of hydrogen isotope, P_X (Pa), in each channel:

$$J_X = D_X S_X\left(\sqrt{P_{X_1}} - \sqrt{P_{X_2}}\right) = K_X\left(\sqrt{P_{X_1}} - \sqrt{P_{X_2}}\right), \tag{4}$$

where S_X ($mol/m^3\ Pa^{1/2}$) is the solubility constant and $K_X = D_X S_X$ (mol m/m^2 s $Pa^{1/2}$) is the permeability.

2.2. Permeation of multi-component hydrogen isotopes system

Eq. (4) derived for the single-component hydrogen isotope system may not be applicable if there exist two or three hydrogen isotopes in the permeation tube because the presence of one hydrogen isotope can influence the solubility of the others [12–15]. Then, the solubilities obtained in the multi-component hydrogen isotopes system must be used in evaluation of the permeation rate using Eq. (2).

The present authors have discussed three patterns for solubilities in the binary-component hydrogen isotopes system in palladium [12]. Following this idea, three patterns of correlation for the permeation rates with solubilities are obtained as follows.

Case I: When each hydrogen isotope acts independently in solution and diffusion, the permeation rates are expressed as follows:

$$J_H = D_H\left(S_H\sqrt{y_{H_1}P_{t_1}} - S_H\sqrt{y_{H_2}P_{t_2}}\right) = K_H\left(\sqrt{y_{H_1}P_{t_1}} - \sqrt{y_{H_2}P_{t_2}}\right), \tag{5}$$

$$J_D = D_D\left(S_D\sqrt{y_{D_1}P_{t_1}} - S_D\sqrt{y_{D_2}P_{t_2}}\right) = K_D\left(\sqrt{y_{D_1}P_{t_1}} - \sqrt{y_{D_2}P_{t_2}}\right), \tag{6}$$

where P_t (Pa) is the total pressure of hydrogen isotopes and y_X (–) is the mole fraction of hydrogen X_2 in gas phase. These equations are equivalent to Eq. (4), that is, the permeation rates in the binary-component system are expressed by the same way as those in the single-component hydrogen isotope system when this pattern is proper.

Case II: When the ideal solution theory is applied to the absorbed binary mixture in estimation of hydrogen solubilities, the permeation rates are obtained as follows if no interaction of atoms with different isotopes is assumed in the course of diffusion through metal:

$$J_H = D_H\left\{\frac{S_H y_{H_1} + S_D y_{D_1}}{1 + 1/\left[\alpha_{S,H/D}\left(y_{H_1}/y_{D_1}\right)\right]}\sqrt{P_{t_1}} - \frac{S_H y_{H_2} + S_D y_{D_2}}{1 + 1/\left[\alpha_{S,H/D}\left(y_{H_2}/y_{D_2}\right)\right]}\sqrt{P_{t_2}}\right\}, \tag{7}$$

$$J_D = D_D\left\{\frac{S_H y_{H_1} + S_D y_{D_1}}{1 + \alpha_{S,H/D}\left(y_{H_1}/y_{D_1}\right)}\sqrt{P_{t_1}} - \frac{S_H y_{H_2} + S_D y_{D_2}}{1 + \alpha_{S,H/D}\left(y_{H_2}/y_{D_2}\right)}\sqrt{P_{t_2}}\right\}, \tag{8}$$

where $\alpha_{S,H/D}$ (–) is the separation factor in solubility. When this case is proper, the value of the separation factor obtained in the mixture of hydrogen isotopes is different from the value of the isotope effect ratio obtained in the single-component hydrogen isotope system. We have reported recently that the permeation behavior of H_2–D_2 mixture through a membrane of palladium–silver alloy is expressed by the above equations in the case when diffusion controls the permeation [13].

Case III: When the Henry's law is applied to each component of the absorbed binary mixture in estimation of the solubilities of hydrogen isotopes, the permeation rates are expressed as follows:

$$J_H = D_H\left(S_H y_{H_1}\sqrt{P_{t_1}} - S_H y_{H_2}\sqrt{P_{t_2}}\right) = K_H\left(y_{H_1}\sqrt{P_{t_1}} - y_{H_2}\sqrt{P_{t_2}}\right), \tag{9}$$

$$J_D = D_D(S_D y_{D_1}\sqrt{P_{t_1}} - S_D y_{D_2}\sqrt{P_{t_2}} = K_D\left(y_{D_1}\sqrt{P_{t_1}} - y_{D_2}\sqrt{P_{t_2}}\right). \tag{10}$$

This case is the special pattern of case II obtained when the separation factor in solubility, $\alpha_{S,H/D}$, is equal to the isotope effect ratio, $\beta_{S,H/D} = S_H/S_D$ (–). Ackerman assumed this pattern in permeation of the H_2–D_2 binary-component system through a palladium–silver alloy membrane [15].

If case I or III is proper for a certain metal–hydrogen system, the permeation rates of hydrogen isotopes in the multi-component system can be estimated by using the permeabilities determined from the single-component permeation experiments, though measurement of the separation factors in advance is necessary if case II is proper. Accordingly, it is required to check which pattern of solubility is applicable to a certain hydrogen permeable metal.

2.3. Permeation of hydrogen isotopes through long tube

It is difficult to define the average driving force in the multi-component hydrogen permeation when a long permeation tube is used because not only the difference of partial pressure of hydrogen isotopes between inner and outer channels, but also the relative pressure of hydrogen isotopes in the axial direction in each channel changes. It is necessary to note that Eq. (2) is applied when the partial pressures of hydrogen on both side of a permeation tube are taken to be uniform. Then, the overall permeation rate, the averaged value over a permeation tube, is to be estimated applying the numerical calculation with the mass balance equations for each finite element as stated below.

The numerical calculation model of permeation in this study is made on the following six assumptions. (1) The composition of the process gas flowing down each channel of the permeation test section varies with position but not with time (steady-state permeation). (2) The plug flow type mixing is applied to each channel. (3) The flow rate of the process gas is constant and the pressure loss is negligible. (4) The pressure change of the process gas due to permeation is small and can be negligible. (5) The temperature is constant in a finite element. (6) Linear concentration profile across the metal thickness is developed for each hydrogen isotope.

Fig. 1 shows a simple diagram of the numerical calculation model for permeation which corresponds to the permeation test section used in this experiment. The permeation test section is divided into N finite elements and each element has a permeation area of $\Delta A = A/N$ (m^2). The molar flow rates of hydrogen isotopes at the inlet of each channel are h_0 (mol/s) for H_2 and d_0 (mol/s) for D_2 and that at the exit of each channel are h_N (mol/s) and d_N (mol/s). Then, the mass balance in the n-th element are expressed as follows:

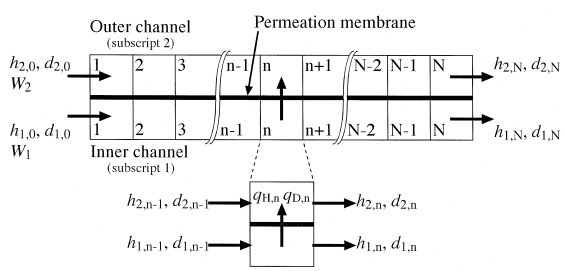

Fig. 1. Schematic diagram of permeation test section as viewed by the numerical calculation model.

$$h_{1,n-1} = h_{1,n} + q_{H,n}, \tag{11}$$

$$d_{1,n-1} = d_{1,n} + q_{D,n}, \tag{12}$$

$$h_{2,n-1} = h_{2,n} - q_{H,n}, \tag{13}$$

$$d_{2,n-1} = d_{2,n} - q_{D,n}, \tag{14}$$

where $q_{X,n}$ (mol/s) is the molar flow rate of hydrogen permeating through the wall of the nth element, and the next equation is led from Eq. (2),

$$q_{X,n} = J_{X,n}\Delta A/t. \tag{15}$$

$J_{X,n}$ (mol m/m^2s) must be replaced by Eqs. (5)–(10) according to the pattern in solubility of hydrogen isotopes in the binary-component system. The overall permeation rates of hydrogen isotopes, $\bar{J}_X$, are expressed as follows:

$$\bar{J}_H = (1/N)\sum_{n=1}^{N} J_{H,n} = (t/A)\sum_{n=1}^{N} q_{H,n} = (h_{1,0} - h_{1,N})t/A = (h_{2,N} - h_{2,0})t/A, \tag{16}$$

$$\bar{J}_D = (1/N)\sum_{n=1}^{N} J_{D,n} = (t/A)\sum_{n=1}^{N} q_{D,n} = (d_{1,0} - d_{1,N})t/A = (d_{2,N} - d_{2,0})t/A. \tag{17}$$

By assuming the ideal gas condition, the molar flow rates of hydrogen isotopes are expressed as follows:

$$h = P_H W/RT, \tag{18}$$

$$d = P_D W/RT, \tag{19}$$

where W (m^3/s) is the flow rate of the process gas, R (J/mol K) is the gas constant, and T (K) is the absolute temperature.

From experiments of the single-component permeation, we get the molar flow rate of a hydrogen isotope at the exit of each channel of the permeation test section (h_N or d_N) when we set the molar flow rate of a hydrogen isotope to each channel (h_0 or d_0), the flow rate of process gas to each channel (W), the operating temperature (T), the permeation tube area (A), and the wall thickness (t). Then, the permeability (K) for each experiment, that is the unknown value, is decided by the fitting method using Eqs. (11)–(17) by computer calculation.

In H_2–D_2 binary-component permeation experiments, the observed overall permeation rates of hydrogen isotopes, $\bar{J}_X = Q_X t/A$, are compared with the calculated values applying Eqs. (5)–(17). Then, we discuss which

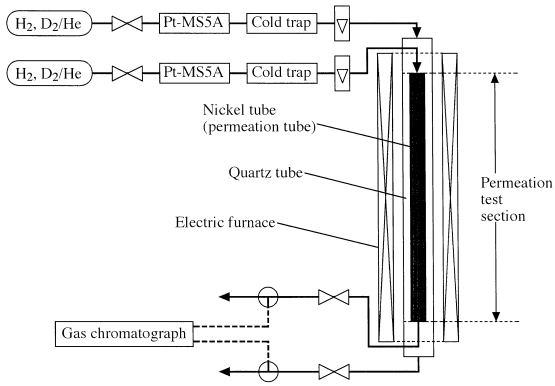

Fig. 2. Schematic diagram of experimental apparatus.

pattern of solubility is applicable to the permeation behavior of the binary-component hydrogen isotopes system.

3. Experimental

Fig. 2 shows a schematic diagram of the experimental apparatus of this study. The experimental conditions are shown in Table 1. A tube of nickel with a nominal purity of 99% (230 mm long, 12.0 mm outer diameter, and 11.0 mm inner diameter, purchased from Nilaco) was concentrically placed in a quartz tube (22.0 mm inner diameter) and copper tubes and brass joints were used as the piping materials of this experimental apparatus. Helium gas with H_2 or/and D_2 was used as the process gas to the inner and outer flow channels. The flow rate of the process gas to each channel was changed from 0.1 to 0.6 l/min at the standard condition. The process gas was initially passed through the packed bed of Platinum-Molecular Sieves 5A (Pt-MS5A) catalyst to change residual oxygen to water. Then, the process gas was passed through the cold trap packed with glass beads and immersed in liquid nitrogen to exclude water before introduction to the permeation test section. The total pressure of the process gas was kept at the atmospheric pressure because pressure difference between inlet and exit end of the permeation test section was measured to be negligible by a pressure gauge. Temperature of the permeation membrane was changed from 473 to 973 K using an electric furnace. The partial pressure of H_2 or/and D_2 in the process gas at inlet was changed from 22.3 to 10^5 Pa in this study.

The permeation rates were measured by the steady-state method and the experiments were carried out as follows. First, helium gas with about 20% H_2 was passed through both channels of the permeation test section and the test section was heated up stepwise to 973 K to activate the permeation membrane. Second the temperature of the test section was set to the experimental temperature and the experimental feed gas was passed through the test section until the permeation of hydrogen isotopes reached the steady state. Then, the concentration of hydrogen isotopes at inlet and outlet of both channels was measured by gas chromatography.

4. Results and discussion

4.1. Permeation of single-component hydrogen isotope

The following equations are obtained for the permeabilities of H_2 and D_2 through nickel in the single-component

Table 1
Experimental conditions

Run number	Channel	Inlet partial pressure of hydrogen isotope(s)		Flow rate (at STP)	Temperature
Single component system					
Run 1-1	inner	H_2: 32.3–56.4 Pa		0.1–0.6 l/min	473–973 K (200–700°C)
	outer	H_2: 75.4–10^5 Pa		0.1–0.6 l/min	
Run 1-2	inner	D_2: 25.7–41.3 Pa		0.1–0.6 l/min	623–973 K (350–700°C)
	outer	D_2: 97.5–6170 Pa		0.1–0.6 l/min	
Binary component system					
Run 2-1	inner	D_2: 6340 Pa		0.2 l/min	623–973 K (350–700°C)
	outer	H_2: 6280 Pa		0.2 l/min	
Run 2-2	inner	D_2: 193 Pa		0.2 l/min	973 K (700°C)
	outer	H_2: 25.8–19500 Pa		0.2 l/min	
Run 2-3	inner	H_2: 190 Pa		0.2 l/min	973 K (700°C)
	outer	D_2: 22.3–2068 Pa		0.2 l/min	
Run 2-4	inner	D_2: 29.3–6460 Pa	H_2:D_2 ≒1:1	0.2 l/min	973 K (700°C)
	outer	H_2: 28.7–6210 Pa		0.2 l/min	
Run 2-5	inner	H_2: 197 Pa		0.2 l/min	973 K (700°C)
	outer	H_2: 224–3990 Pa; D_2: 232–3870 Pa	H_2:D_2 ≒1:1	0.2 l/min	

permeation experiments of this study,

$$K_H = 4.44 \times 10^{-7} \exp(-5.48 \times 10^4 / RT), \quad (20)$$

$$K_D = 3.81 \times 10^{-7} \exp(-5.62 \times 10^4 / RT). \quad (21)$$

These equations are shown in Figs. 3 and 4. Fig. 5 shows a comparison of estimated permeation rates averaged over the permeation tube with observed values estimated from the partial pressure difference between inlet and outlet of the permeation test section. Good agreement shown in this figure indicates that the method of calculation described in Section 2.3 is reasonable to estimate the amount of permeation.

Permeabilities obtained in this study are compared in Figs. 3 and 4 with reported values [1–8]. The apparent activation energy of H_2 or D_2 permeation obtained in this study, 54.8 kJ/mol for H_2 and 56.2 kJ/mol for D_2, is almost equal to the activation energies reported by various authors as can be seen from these figures. The permeability of H_2 obtained in this study is close to the values reported by Ebisuzaki et al. [2], Eichenauer et al. [3], or Robertson [6] and the permeability of D_2 in this study to the values by Ebisuzaki et al. [2,8] or Eichenauer et al. [3]. Because Ebisuzaki et al. did not give the D_2 permeability in their reports, the value shown in Fig. 4 is estimated from their data on H_2 permeability [2] and isotope effect ratio [8]. Although some authors have reported [1,5] that there was a discontinuous change in permeability in the vicinity of the Curie point (623 ± 10 K for nickel), however, such a change was not observed in this study.

The isotope effect ratio in permeation, $\beta_{P,H/D}$, is obtained as follows, where the isotope effect ratio is defined

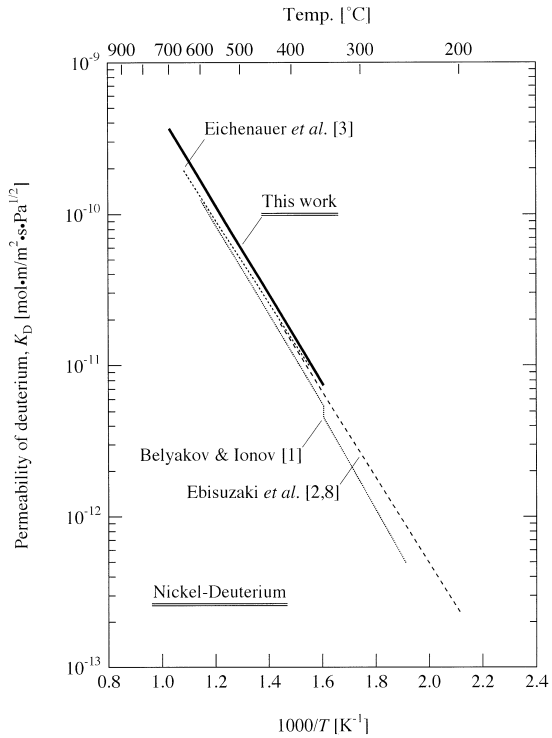

Fig. 4. Temperature dependence of the deuterium permeability through nickel.

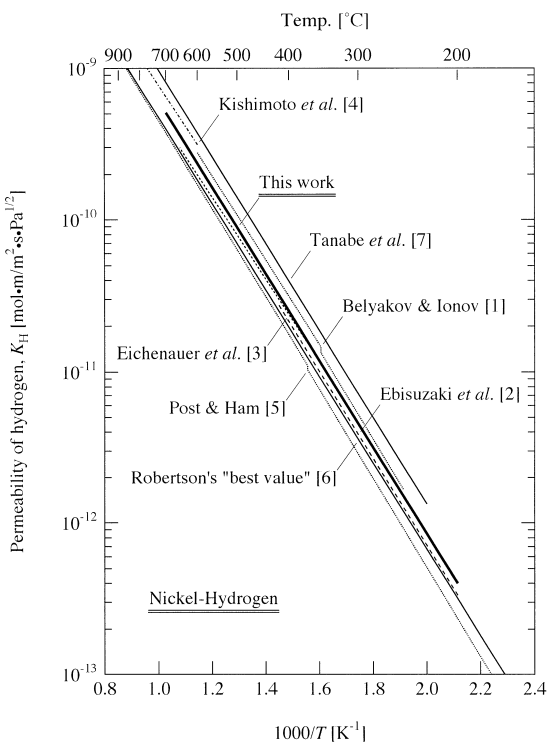

Fig. 3. Temperature dependence of the hydrogen permeability through nickel.

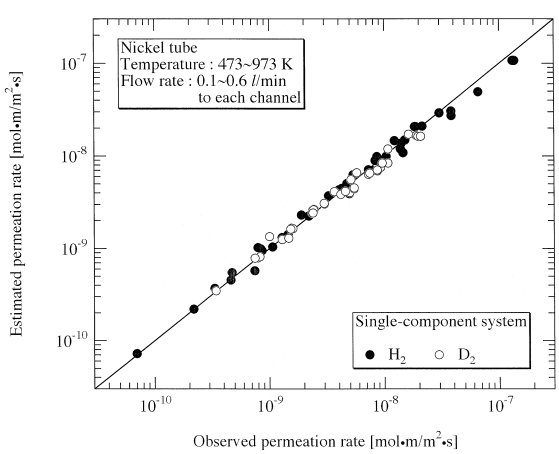

Fig. 5. Comparison of estimated permeation rates with observed values for single-component hydrogen isotope system.

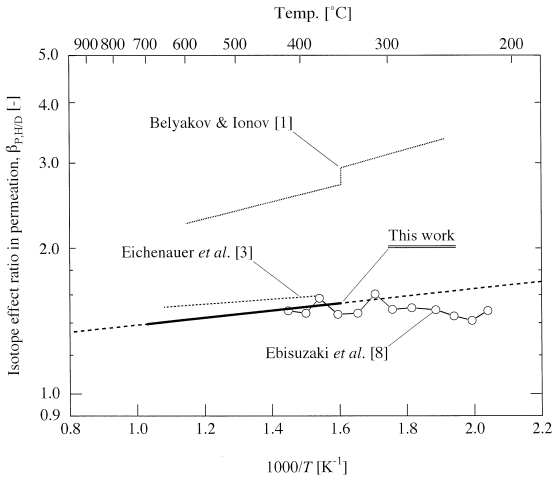

Fig. 6. Temperature dependence of the isotope effect ratio in permeation through nickel.

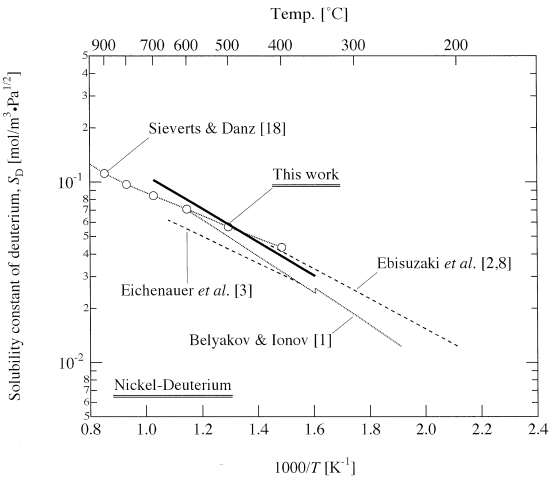

Fig. 8. Temperature dependence of the relevant deuterium solubility constant in nickel.

as the ratio of properties of each isotope observed in the single component experiment:

$$\beta_{P,H/D} = K_H/K_D = 1.16\exp\left(1.4\times10^3/RT\right), \quad (22)$$

and shown in Fig. 6 with the reported values [1,3,8]. The isotope effect ratio in permeation of this study varies from 1.38 at 973 K to 1.52 at 623 K and is similar to the values reported by Eichenauer et al. [3] and Ebisuzaki et al. [8]. The isotope effect ratio of $\sqrt{2}$, that is said to be the ideal value of isotope effect ratio on permeation, is obtained at 850 K from Eq. (22).

We calculate the relevant solubility constants from the permeabilities obtained in this study and a set of diffusivities reported by Völkl and Alefeld [16] as

$$S_H = 0.643\exp\left(-1.43\times10^4/RT\right), \quad (23)$$

$$S_D = 0.906\exp\left(-1.76\times10^4/RT\right). \quad (24)$$

Solubility constants represented by above equations are comparable with the reported values by various authors [1–3,6–8,17,18] as shown in Figs. 7 and 8, and they are almost equal to the values reported by Ebisuzaki et al. [2,8].

When the temperature distribution is formed along the axial direction of the permeation tube as shown in Fig. 9, it is presumed from Eq. (20) that the local permeability of H_2, $K_H(z)$, distributes in the manner as shown in the same figure, where z (m) is the distance from entrance of the permeation tube. The temperature distribution is measured by the thermocouples placed at intervals of 1.0 cm along the axial direction of the permeation tube. In this example of the temperature distribution, the maximum temperature, T_{max}, is observed to be 873 K at the center of the permeation tube and the minimum temperature, T_{min}, 681 K at the inlet of that. Longhurst et al. [19] have

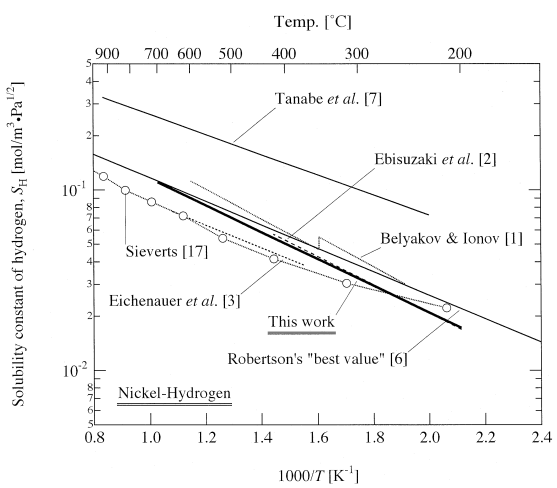

Fig. 7. Temperature dependence of the relevant hydrogen solubility constant in nickel.

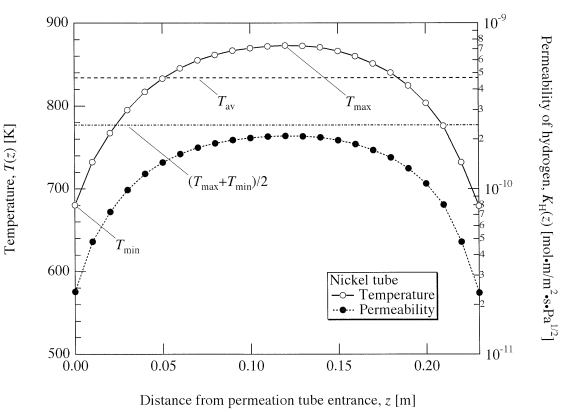

Fig. 9. Distributions of temperature and local permeability of hydrogen as a function of distance from permeation tube entrance.

Table 2
Comparison of observed value with estimated values under various temperature distributions

Experimental conditions			
Membrane		Nickel: length, 230 nm; outer diameter, 12.0 mm; inner diameter, 11.0 mm	
Inlet partial pressure of H_2		54.4 Pa (inner channel); 2860 Pa (outer channel)	
Flow rate		0.2 l/min to each channel	
Temperature distribution		$T(z)$ shown in Fig. 9	
Observed permeation quantity, Q_{ob}		1.14×10^{-7} mol/s	
Representative temperature for permeation		Estimated permeation quantity, Q_{est}	Error $= 100 \times (Q_{est} - Q_{ob})/Q_{ob}$
No. 1	$T_{max} = 873$ K constant	1.65×10^{-7} mol/s	+44.7%
No. 2	$T_{min} = 681$ K constant	2.09×10^{-8} mol/s	−81.7%
No. 3	$(T_{max} + T_{min})/2 = 777$ K constant	6.83×10^{-8} mol/s	−40.1%
No. 4	$T_{av} = 834$ K constant	1.19×10^{-7} mol/s	+4.3%
No. 5	$T(z)$ shown in Fig. 9	1.17×10^{-7} mol/s	+2.6%

proposed to use the average temperature, T_{av} (K), as follows:

$$\exp(-E/RT_{av}) = (1/l)\int_0^l \exp\{-E/RT(z)\}\,dz, \qquad (25)$$

where E (J/mol) is the activation energy of H_2 permeation, and T_{av} is calculated to be 834 K for the temperature distribution shown in Fig. 9. In Table 2, we compare the permeation quantity observed when the temperature distribution as shown in Fig. 9 was made with the estimated values using five different ways as follows. (1) Use of T_{max} as the representative temperature in numerical calculation method explained in Section 2.3. (2) Use of T_{min} as the representative temperature in numerical calculation. (3) Use of $(T_{max} + T_{max})/2$ as the representative temperature in numerical calculation. (4) Use of T_{av} as the representative temperature in numerical calculation. (5) Use of local temperature to each finite section of permeation tube in numerical calculation.

Agreement between the observed value and the calculated value using the way of No. 4 or 5 is quite good in comparison with the calculated value using the way of No. 1, 2, or 3. From this comparison it is concluded that the average temperature of permeation tube is well represented by Eq. (25). However, it may not be necessary to use the average temperature intentionally to each finite section in numerical calculation. In the case where the concentration difference between inlet and outlet is larger than the case compared above, use of T_{av} gives more error. Accordingly, we recommend to use the way of No. 5. Comparison in Table 2 implies that improper selection of the representative temperature for permeation is one of the main reasons for scattering of reported permeabilities shown in Figs. 3 and 4, since there must exist the temperature distribution in a permeation membrane.

4.2. Permeation of multi-component hydrogen isotopes

The experimental overall permeation rates of hydrogen isotopes observed when both H_2 and D_2 are introduced to the permeation test section are shown in Figs. 10–12 with estimated values, where estimation is performed assuming applicability of case I or III for the solubility of hydrogen isotopes in nickel at the binary-component hydrogen isotopes system.

Fig. 10 shows the dependence of the overall permeation rates of H_2 and D_2 on the inlet partial pressure of H_2 introduced to the outer channel while the inlet partial pressure of D_2 to the inner channel was kept constant at 193 Pa. Fig. 10 shows that the overall permeation rate of D_2 to the outer channel increases with addition of hydrogen to the outer channel by about 15% at the maximum, although it becomes smaller than the permeation rate observed at the single-component D_2 permeation when the partial pressure of H_2 in the process gas to the outer channel exceeds several thousands pascals. Permeation of D_2 shows maximum when the partial pressure of H_2 in the process gas introduced to the outer channel is 350 Pa. As

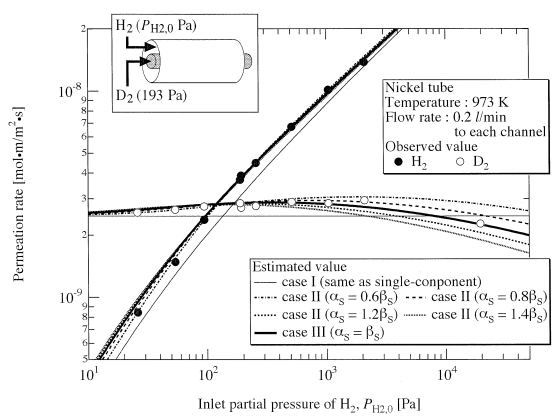

Fig. 10. The dependence of the permeation rates of H_2 and D_2 on the inlet partial pressure of H_2 introduced to the outer channel. The inlet partial pressure of D_2 to the inner channel was kept constant at 193 Pa.

can be seen from this figure the overall permeation rate of H_2 through the nickel wall becomes also larger than the permeation rate observed at the single component H_2 permeation by about 30% in this experimental range. The estimated values assuming applicability of case II are also compared with the observed values in Fig. 10 where the separation factor in solubility is taken as the parameter. It is seen from Fig. 10 that application of case III to the solubility of hydrogen isotopes in nickel is proper because the estimated permeation rates using case III agree well with the observed overall permeation rates.

Fig. 11 shows the partial pressure dependence of the permeation rates observed when helium with H_2 was introduced to the outer channel and helium with D_2 of the same partial pressure as H_2 to the inner channel. It is seen from this figure that the overall permeation rate of H_2 or D_2 becomes larger than the value observed at the single-component system when the other hydrogen isotope is introduced to the other channel. It can be also seen from this figure that the observed overall permeation rate agree with the estimated values assuming the applicability of case III to the solubility at the binary-component hydrogen isotopes system.

Fig. 12 shows the overall permeation rates observed under the conditions where the inlet partial pressure of D_2 to the inner channel was kept at 197 Pa and the inlet partial pressure of the mixture of H_2 and D_2 in the process gas to the outer channel were changed keeping the relative pressure as unity. No permeation is expected when the inlet partial pressure of D_2 in the process gas to the outer channel is equal to the inlet partial pressure of D_2 to the inner channel, that is, 197 Pa as shown by dashed lines in Fig. 12 if application of case I is proper. However, no permeation is expected when the inlet partial pressure of D_2 to the outer channel is 332 Pa as shown by dotted lines if application of case III is proper. The observed values

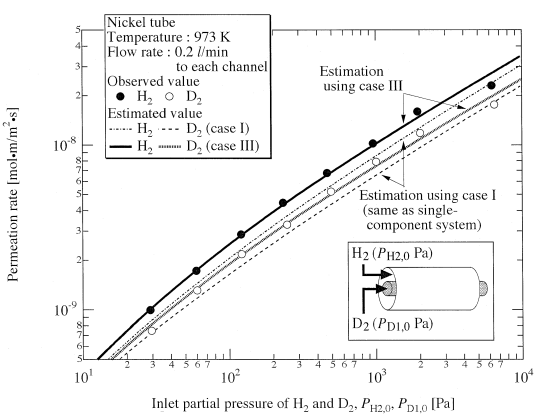

Fig. 11. The partial pressure dependence of the permeation rates of H_2 and D_2 observed under the conditions where helium with H_2 was introduced to the outer channel and helium with D_2 of the same partial pressure as hydrogen to inner channel.

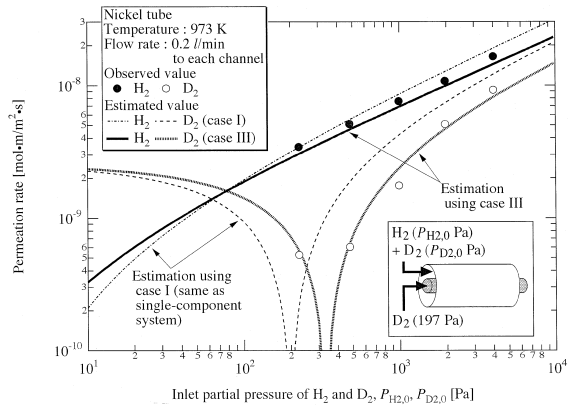

Fig. 12. The dependence of the permeation rates of H_2 and D_2 on the inlet partial pressure of the mixture of H_2 and D_2 introduced to the outer channel keeping the relative pressure as unity. The inlet partial pressure of D_2 to the inner channel was kept constant at 197 Pa.

shown in this figure are represented well by the dotted lines.

Accordingly, it can be said that the permeation behavior of binary-component hydrogen isotopes through nickel is expressed assuming that the separation factor in solubility is the same as the isotope effect ratio and that diffusivities obtained at the single-component diffusion measurement is applicable to the binary-component diffusion. The reason for these is that the interaction between hydrogen and deuterium is small because of the small solubility of hydrogen isotopes in nickel. (H/Ni is 2.9×10^{-4} at 773 K and 1.0×10^5 Pa of H_2.) On the other hand, we have reported that the separation factor is different from the isotope effect ratio in such material as palladium which has large solubility of hydrogen isotopes [12]. (H/Pd is 6.8×10^{-3} at 773 K and 1.0×10^5 Pa of H_2.) The authors consider that further discussions with more data on the solubility of multi-component hydrogen isotopes system are necessary. It can be also said that the numerical calculation model described in Section 2.3 of this study is proper to estimate the permeation behaviors of hydrogen isotopes in the piping system under various conditions.

Profiles of the partial pressure of hydrogen isotopes in the axial direction of a nickel permeation tube are numerically estimated and shown in Figs. 13–15 as a function of distance from the inlet of the permeation tube. In these calculations use of the same permeation tube as that used in this experiment is assumed.

In Fig. 13 the inlet partial pressure of D_2 to the inner channel is assumed to be 1.0 Pa and that of H_2 to the outer channel is changed from 0 to 100 Pa, and the flow rate of the process gas to each channel is 0.05 l/min.

On permeation of the binary-component hydrogen iso-

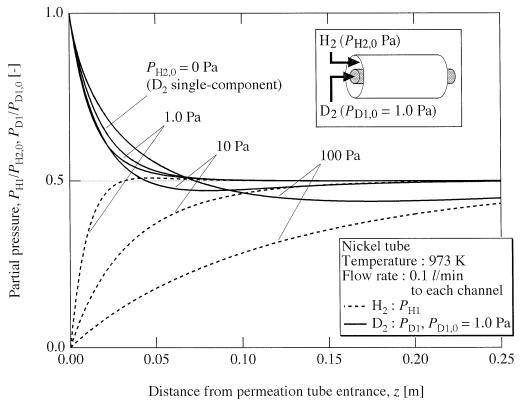

Fig. 13. The model calculations of H_2 and D_2 partial pressure profiles in the inner channel as a function of distance from the permeation tube entrance. The inlet partial pressure of D_2 to the inner channel is kept constant at 1.0 Pa and that of H_2 to the outer channel is changed from 0 to 100 Pa.

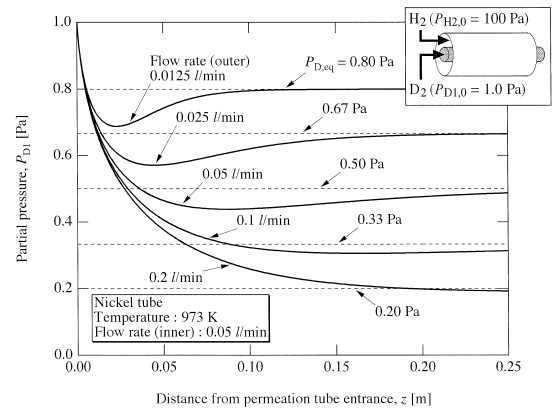

Fig. 14. The model calculations of D_2 partial pressure profiles in the inner channel as a function of distance from the permeation tube entrance. The flow rate of the inner channel is kept constant at 0.05 l/min and that of outer channel is changed from 0.0125 to 0.2 l/min.

topes system, the driving force for permeation of D_2, $\Delta P_D^{1/2}$ ($Pa^{1/2}$), is shown as follows from Eq. (10):

$$\Delta P_D^{1/2} = P_{D_1}/\sqrt{P_{H_1} + P_{D_1}} - P_{D_2}/\sqrt{P_{H_2} + P_{D_2}}. \qquad (26)$$

Accordingly, D_2 permeates from inner to outer channel even when P_{D_2} is larger than P_{D_1} if the total pressure of hydrogen isotopes in the outer channel is larger than that in the inner channel. For example, permeation of D_2 from inner to outer channel occurs when $P_{D_1} = 1$ Pa, $P_{H_1} = 3$ Pa, and $P_{D_2} = 10$ Pa if P_{H_2} is larger than 390 Pa.

It is shown in Fig. 13 that more than half of D_2 introduced to the inner channel is transferred to the outer channel when the partial pressure of H_2 to the outer channel is larger than 10 Pa. This effect is ascribed to the effect of H_2 permeated from the outer channel. The more is H_2 to the outer channel, the less is the driving force for permeation of D_2 to the outer channel, although addition of a small amount of H_2 to the outer channel promotes the permeation of D_2 from the inner channel because assumption of case III is applied to solubilities of hydrogen isotopes in nickel.

The estimations shown in Fig. 13 do not affirm the idea to introduce hydrogen to the outer channel of a double tube for prevention of tritium leakage from the inner channel. If the permeation tube is long enough, the partial pressures of H_2 and D_2 in the inner channel reach equilibrium with the partial pressures in the outer channel.

Fig. 14 shows the changes of the profiles of D_2 partial pressure in the inner channel with the flow rates of the outer channel in the case where the inlet partial pressure of D_2 to the inner channel is assumed to be 1.0 Pa and that of H_2 to the outer channel is 100 Pa. As the flow rate of the outer channel becomes larger, the equilibrium partial pressure of D_2 becomes lower. The partial pressures of H_2 and D_2 in the inner channel are equal to that in the outer channel at the equilibrium condition. The equilibrium partial pressure of hydrogen X_2, $P_{X,eq}$ (Pa), is shown as follows using Eqs. (11)–(14), (18) and (19):

$$P_{X,eq} - \left(P_{X_1,0}W_1 + P_{X_2,0}W_2\right)/(W_1 + W_2), \qquad (27)$$

where $P_{X,0}$ (Pa) is the inlet partial pressure of X_2. $P_{X,eq}$ is expressed by the inner and outer flow rates of the process gas and the inlet partial pressure of hydrogen X_2.

Profiles of the partial pressure of hydrogen isotopes in the axial direction of a nickel permeation tube are calculated for the three-component hydrogen isotopes system with H_2, D_2, and T_2 where observations obtained at the

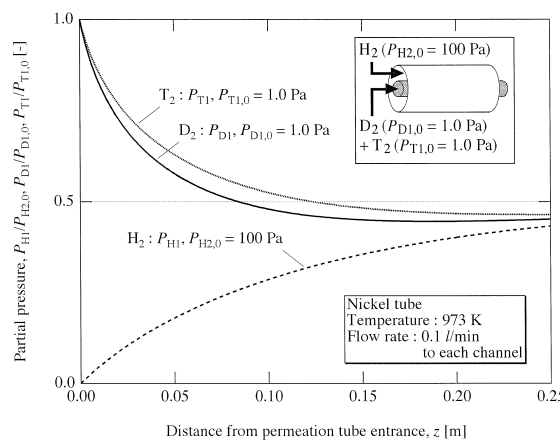

Fig. 15. The model calculations of H_2, D_2, and T_2 partial pressure profiles in the inner channel as a function of distance from the permeation tube entrance. The inlet partial pressure of D_2 and T_2 to the inner channel are 1.0 Pa and that of H_2 to the outer channel is 100 Pa.

binary-component system are assumed to be applicable to the three-component system. In this calculation permeability of T_2, K_T, is assumed to be $\sqrt{2/3}$. When H_2 of 100 Pa is added to the process gas to the outer channel while the mixture of D_2 of 1.0 Pa and T_2 of 1.0 Pa goes into the inner channel, tritium permeates through the nickel wall following deuterium as can be seen from Fig. 15. More than half of tritium and deuterium temporarily leave the inner channel when a large amount of hydrogen is added to the outer channel.

5. Conclusions

The permeabilities of H_2 and D_2 through nickel are quantified and they agree well with previously reported values. The solubilities of H_2 and D_2 for nickel calculated from the permeabilities of this study and the diffusivities of the literature data also agree well with previously reported values.

The permeation behavior of hydrogen isotopes through nickel in the binary-component hydrogen isotopes system are observed and compared with the values from the model calculation. It is concluded in this study that the numerical calculation is to be applied to predict the permeation behavior of hydrogen isotopes through the wall of a long tube especially when the mixtures of hydrogen isotopes are treated. It is also observed in this study that the separation factor in permeation through nickel obtained from the binary-component hydrogen isotopes system coincides with the isotope effect ratio obtained from the single-component hydrogen isotope system.

References

[1] Y.I. Belyakov, N.I. Ionov, Sov. Phys.-Tech. Phys. 6 (1961) 146.
[2] Y. Ebisuzaki, W.J. Kass, M. O'Keeffe, J. Chem. Phys. 46 (1967) 1378.
[3] W. Eichenauer, W. Löser, H. Witte, Z. Metallkd. 56 (1965) 287.
[4] N. Kishimoto, T. Tanabe, H. Araki, H. Yoshida, R. Watanabe, Nucl. Technol. 66 (1984) 578.
[5] C.B. Post, W.R. Ham, J. Chem. Phys. 6 (1938) 598.
[6] W.M. Robertson, Z. Metallkd. 64 (1973) 436.
[7] T. Tanabe, Y. Yamanishi, K. Sawada, S. Imoto, J. Nucl. Mater. 122&123 (1984) 1568.
[8] Y. Ebisuzaki, W.J. Kass, M. O'Keeffe, J. Chem. Phys. 46 (1967) 1373.
[9] J.T. Bell, J.D. Redman, J. Chem. Phys. 82 (1978) 2834.
[10] K.J. Gorman, W.R. Nardella, Vacuum 12 (1962) 19.
[11] A.D. Le Claire, Diffus. Def. Data 35 (1984) 1.
[12] M. Nishikawa, T. Shiraishi, K. Murakami, J. Nucl. Sci. Technol. 33 (1996) 504.
[13] M. Nishikawa, T. Shiraishi, Y. Kawamura, T. Takeishi, J. Nucl. Sci. Technol. 33 (1996) 774.
[14] R.G. Hickman, J. Less-Common Met. 19 (1969) 369.
[15] F.J. Ackerman, G.J. Koskinas, Ind. Eng. Chem. Fundam. 11 (1972) 332.
[16] J. Völkl, G. Alefeld, Hydrogen in Metals I, Springer, Berlin, 1978.
[17] A. Sieverts, Z. Metallkd. 21 (1929) 41.
[18] A. Sieverts, W. Danz, Z. Metallkd. 247 (1941) 131.
[19] G.R. Longhurst, G.A. Deis, P.Y. Hsu, L.G. Miller, R.A. Causey, Nucl. Technol./Fusion 4 (1983) 681.